HHS Public Access

Author manuscript

*Oral Dis*. Author manuscript; available in PMC 2019 July 22.

Published in final edited form as:

*Oral Dis*. 2018 July ; 24(5): 761–771. doi:10.1111/odi.12823.

# $P2Y_2R$ deletion ameliorates sialadenitis in IL-14α-transgenic mice

**LT Woods**[1,2], **JM Camden**[1,2], **MG Khalafalla**[1,2], **MJ Petris**[1,2,3], **L Erb**[1,2], **JL Ambrus Jr**[4], **GA Weisman**[1,2]

[1]Department of Biochemistry, University of Missouri, Columbia, MO, USA

[2]Christopher S. Bond Life Sciences Center, University of Missouri, Columbia, MO, USA

[3]Department of Nutritional Sciences and Exercise Physiology, University of Missouri, Columbia, MO, USA

[4]Department of Medicine, Division of Allergy, Immunology and Rheumatology, SUNY at Buffalo School of Medicine and Biomedical Sciences, Buffalo, NY, USA

## Abstract

**Objective—**Interleukin-14α-transgenic (IL-14αTG) mice develop an autoimmune exocrinopathy with characteristics similar to Sjögren's syndrome, including sialadenitis and hyposalivation. The $P2Y_2$ receptor ($P2Y_2R$) for extracellular ATP and UTP is up-regulated during salivary gland inflammation (i.e., sialadenitis) where it regulates numerous inflammatory responses. This study investigated the role of $P2Y_2Rs$ in autoimmune sialadenitis in the IL-14αTG mouse model of Sjögren's syndrome.

**Materials and Methods—**IL-14αTG mice were bred with $P2Y_2R^{-/-}$ mice to generate IL-14αTG × $P2Y_2R^{-/-}$ mice. $P2Y_2R$ expression, lymphocytic focus scores, B- and T-cell accumulation, and lymphotoxin-α expression were evaluated in the submandibular glands (SMG) along with carbachol-stimulated saliva secretion in IL-14αTG, IL-14αTG × $P2Y_2R^{-/-}$, and C57BL/6 control mice at 9 and 12 months of age.

**Results—**Genetic ablation of $P2Y_2Rs$ in IL-14αTG mice significantly reduced B and T lymphocyte infiltration of SMGs. However, reduced sialadenitis did not restore saliva secretion in IL-14αTG × $P2Y_2R^{-/-}$ mice. Decreased sialadenitis in IL-14αTG × $P2Y_2R^{-/-}$ mice correlated with decreased lymphotoxin-α levels, a critical proinflammatory cytokine associated with autoimmune pathology in IL-14αTG mice.

**Correspondence** Gary A. Weisman, Department of Biochemistry, 540E Life Sciences Center, University of Missouri, Columbia, MO, USA. weismang@missouri.edu.

AUTHOR CONTRIBUTIONS

LTW, JMC and MGK contributed to study conception and design, performed experiments, analyzed data and interpreted data. MJP, LE, JLA and GAW contributed to study conception and design and data interpretation. LTW drafted the manuscript and all authors critically revised the manuscript.

CONFLICT OF INTERESTS

None to declare.

SUPPORTING INFORMATION

Additional Supporting Information may be found online in the supporting information tab for this article.

**Conclusions—**The results of this study suggest that $P2Y_2Rs$ contribute to the development of salivary gland inflammation in IL-14αTG mice and may also contribute to autoimmune sialadenitis in humans.

**Keywords**

autoimmunity; lymphotoxin-alpha; nucleotides; purinergic receptors; salivary glands; Sjögren's syndrome

## 1 | INTRODUCTION

One commonality between many human diseases is chronic inflammation, a process by which cells of the immune system persistently infiltrate diseased or damaged tissue. In chronic inflammation, sustained accumulation of immune cells exacerbates tissue degeneration in diseases such as Sjögren's syndrome (SS), an autoimmune exocrinopathy of the salivary and lacrimal glands (Mavragani & Moutsopoulos, 2014). Diagnostic criteria for SS include the presence in blood serum of autoantibodies against the ribonucleoproteins Ro/SSA and La/SSB (or positive rheumatoid factor and antinuclear antibody titers ≥ 1:320), an ocular dye staining score > 3, and focal lymphocytic sialadenitis (focus score ≥ 1 per 4 $mm^2$), as determined by histopathology of a minor salivary gland tissue biopsy (Shiboski et al., 2012). Current therapeutic options for SS are limited to symptom management with topical agents to improve moisture (i.e., artificial saliva or tears) and cholinergic agents to promote saliva secretion from residual salivary acinar cells. There is a critical need for more effective therapies that treat the underlying chronic inflammation in autoimmune diseases, such as SS, where short-circuiting a systemic autoimmune response could prevent the damaging effects of chronic inflammation.

Studies from our laboratory and others have implicated extracellular nucleotides, such as ATP, as initiators of inflammation in SS (Ahn, Camden, Schrader, Redman, & Turner, 2000; Turner, Weisman, & Camden, 1997; Woods et al., 2012). Among the P2 purinergic receptors for extracellular nucleotides, including the ATP-gated ionotropic P2X receptors (P2X1–7) and the G protein-coupled P2Y receptors ($P2Y_{1,2,4,6,11,12,13,14}$) for adenine and uridine nucleotides, the P2X7 and $P2Y_2$ receptors have been shown to be initial responders to nucleotides released during salivary gland inflammation (Ahn et al., 2000; Schrader, Camden, & Weisman, 2005; Turner et al., 1997; Woods et al., 2012). The $P2Y_2$ receptor ($P2Y_2R$), which responds equipotently to ATP and UTP, is distinguished by the fact that it is upregulated in inflamed or damaged tissues, most likely due to NF-κB-mediated *$P2Y_2R$* gene transcription in response to inflammatory agents produced in part by P2X7 receptor activation by ATP (Ahn et al., 2000; Degagne et al., 2009; Schrader et al., 2005; Turner et al., 1997). In salivary glands, the $P2Y_2R$ is upregulated in rodent primary submandibular gland (SMG) epithelial cells during short-term culture (El-Sayed et al., 2014; Turner et al., 1997) and in response to duct ligation-induced SMG inflammation (Ahn et al., 2000). Additionally, we have shown selective upregulation of the $P2Y_2R$, but not other uridine nucleotide receptors (i.e., $P2Y_4R$ or $P2Y_6R$), in SMG cells from the NOD.B10 mouse model of SS (Schrader et al., 2005) and observed $P2Y_2R$ upregulation in SMGs isolated from the C57BL/6-NOD.Aec1Aec2 SS mouse model (unpublished observations; (Cha, Nagashima,

Brown, Peck, & Humphreys-Beher, 2002)). Upon activation, $P2Y_2Rs$ stimulate canonical $G_q\alpha$ signaling (i.e., increased phospholipase C activity leading to inositol 1,4,5 trisphosphate and diacylglycerol production and subsequent elevations in $[Ca^{2+}]_i$ and protein kinase C activation, respectively (Lustig et al., 1992)), as well as numerous signaling pathways that regulate inflammatory processes, including metalloprotease activation, growth factor receptor transactivation, and interaction with $\alpha_v\beta_{3/5}$ integrins (Bagchi et al., 2005; Ratchford et al., 2010; Seye, Yu, Gonzalez, Erb, & Weisman, 2004). Notably, the C-terminus of the $P2Y_2R$ also interacts with the actin-binding protein filamin A that, along with RhoA activation, increases the release of lymphotoxin-α (LTA), a proinflammatory cytokine and key regulator of sialadenitis in the interleukin-14α-transgenic (IL-14αTG) mouse model of SS (Seye, Agca, Agca, & Derbigny, 2012; Shen et al., 2010, 2013).

The IL-14αTG mouse model of SS recapitulates many of the autoimmune pathologies associated with SS development in humans and was generated by overexpressing human IL-14α in C57BL/6 mice (Shen et al., 2006). In the human genome, the IL-14α gene (also known as taxilin alpha) has been mapped to an area near a susceptibility region for systemic lupus erythematosus (Gaffney et al., 1998), suggesting that IL-14α plays a role in the development of other autoimmune diseases such as SS (Shen et al., 2006). Indeed, IL-14αTG mice exhibit temporal pathophysiological changes similar to human SS, including decreased saliva flow and lymphocytic infiltration of submandibular, lacrimal, and eventually parotid glands (Shen et al., 2006, 2009, 2010, 2013). As compared to age-matched C57BL/6 control mice, whole saliva production in IL-14αTG mice is significantly decreased by ~6 months of age, and by ~9 months of age, the SMGs exhibit substantial lymphocytic infiltration (Shen et al., 2006, 2009). Severe autoimmune manifestations are evident at ~15 months of age, including the development of $CD5^+$ B-cell lymphomas, consistent with lymphoma development in human SS patients (Shen et al., 2006). Because previous studies have suggested a role for the $P2Y_2R$ in salivary gland inflammation, this study was initiated to define the contributions of the $P2Y_2R$ to salivary gland inflammation in IL-14αTG mice through the generation of IL-14αTG × $P2Y_2R^{-/-}$ mice.

## 2 | MATERIALS AND METHODS

### 2.1 | Mice

IL-14αTG mice were developed by Dr. Julian Ambrus (State University of New York at Buffalo) and have been previously described (Shen et al., 2006, 2009, 2010, 2013). Wild-type C57BL/6 (Stock No. 000664) and $P2Y_2R^{-/-}$ mice (Stock No. 009132) were purchased from Jackson Laboratories (Bar Harbor, ME). IL-14αTG mice were bred with $P2Y_2R^{-/-}$ mice to generate IL-14αTG × $P2Y_2R^{-/-}$ mice. All mice were bred at the Christopher S. Bond Life Sciences Center Animal Facility of the University of Missouri, Columbia, MO. Animals were housed in vented cages with 12-hr light/dark cycles and received food and water ad libitum. Age-matched 9- and/or 12-month-old female mice were utilized for all experiments and were genotyped by PCR using appropriate primers, as previously described (Ajit et al., 2014; Shen et al., 2006). Euthanasia was performed by terminal anesthesia with Avertin (Sigma-Aldrich, St. Louis, MO; 0.75 mg/g mouse weight given intraperitoneally) followed by cervical dislocation with efforts taken to minimize suffering. All experimental

animal procedures were conducted in accordance with National Institutes of Health guidelines and were approved by the University of Missouri Animal Care and Use Committee (Protocol Number 8814).

### 2.2 | Real-time PCR

Real-time PCR (RT-PCR) was performed as previously described (Woods et al., 2015). Briefly, whole SMGs were excised from euthanized mice and homogenized in TRIzol reagent (ThermoFisher Scientific, Waltham, MA). Chloroform (0.2 ml/ml TRIzol) was added, and samples were incubated for 5 min at room temperature. Samples were centrifuged at 12,000 × *g* for 15 min at 4°C, and the resulting aqueous phase was utilized for RNA isolation using the RNeasy Plus Mini Kit (Qiagen, Valencia, CA). cDNA was prepared from purified RNA using RNA to cDNA EcoDry Premix (Clontech Laboratories, Mountain View, CA), and RT-PCR was performed on an Applied Biosystems 7500 Real-Time PCR machine using specific Taqman primers for mouse *$P2Y_2R$, CD20 (Ms4a1), CD3* (*Cd247*), *Lymphotoxin-α,* and *18S* (Applied Biosystems, Foster City, CA). For data analysis, mRNA expression of target genes was normalized to 18S ribosomal RNA as an internal control.

### 2.3 | Isolation of primary SMG epithelial and B cells

For primary SMG epithelial cell isolation, whole SMGs from wild-type, IL-14αTG, or IL-14αTG × $P2Y_2R^{-/-}$ mice were excised, minced with razor blades, and placed in dispersion media (1:1 Dulbecco's modified Eagle's medium (DMEM):Ham's F-12 media containing 50 units/ml collagenase (Worthington Biochemical Corporation, Lakewood, NJ), 400 units/ml hyaluronidase, 1% (w/v) bovine serum albumin (BSA), and 0.2 m mol $L^{-1}$ $CaCl_2$). Dispersion media containing SMG tissues were incubated in a shaking water bath at 37°C under 95% air and 5% $CO_2$ for 40 min with manual dispersion by pipetting every 10 min. Dispersed SMG epithelial cells were then washed in assay buffer (120 m mol $L^{-1}$ NaCl, 4 m mol $L^{-1}$ KCl, 1.2 m mol $L^{-1}$ $KH_2PO_4$, 1.2 m mol $L^{-1}$ $MgSO_4$, 1 m mol $L^{-1}$ $CaCl_2$, 10 m mol $L^{-1}$ glucose, 15 m mol $L^{-1}$ HEPES, 1% (w/v) BSA, pH 7.4), filtered through a 100 μm cell strainer, and resuspended in serum-free 1:1 DMEM:Ham's F-12 media containing 100 units/ml penicillin and 100 μg/ml streptomycin.

For primary B-cell isolation, SMGs and spleens from wild-type, IL-14αTG, and IL-14αTG × $P2Y_2R^{-/-}$ mice were excised, placed in isolation buffer (PBS containing 0.5% (w/v) BSA and 2 m mol $L^{-1}$ EDTA, pH 7.2) and mechanically dispersed in a Seward Stomacher 80 Biomaster laboratory system (5-min dispersion for spleen, 10-min dispersion for SMG). The resulting cell suspension was filtered through a 40-μm cell strainer and pelleted by centrifugation at 4°C, 350 × *g* for 5 min. Cells were resuspended in 2 ml of Red Blood Cell Lysis Buffer (BioLegend, San Diego, CA) and placed on ice for 5 min. The remaining cells were washed with cold isolation buffer, and untouched primary B cells were then purified by negative selection using a mouse B Cell Isolation Kit, MS isolation columns, and a MiniMACS magnetic cell separator (Miltenyi Biotec, San Diego, CA), per manufacturer's protocol.

### 2.4 | Single-cell measurements of intracellular free $Ca^{2+}$ concentration

Primary SMG or B cells from wild-type, IL-14αTG, and IL-14αTG × $P2Y_2R^{-/-}$ mice were adhered to chambered coverslips using Cell-Tak cell adhesive (Corning Inc., Corning, NY) and loaded with the $Ca^{2+}$-sensitive fluorescent dye fura-2 by incubation in assay buffer containing 0.1% (w/v) BSA and 2 μ mol $L^{-1}$ fura-2AM (EMD Biosciences, San Diego, CA) for 30 min at 37°C followed by a 30-min incubation in assay buffer without fura-2AM. UTP-induced changes in the 340/380 nm fluorescence excitation ratio (505 nm emission) were detected using an InCyt Dual-Wavelength Fluorescence Imaging System (Intracellular Imaging, Cincinnati, OH). Resulting fluorescence ratios were converted to $[Ca^{2+}]_i$ (n mol $L^{-1}$) using a standard curve created with solutions containing known concentrations of $Ca^{2+}$. In cells that failed to respond to 100 μ mol $L^{-1}$ UTP, the intracellular $Ca^{2+}$ response to 100 μ mol $L^{-1}$ carbachol or 10 μg/ml goat $F(ab')_2$ antimouse IgM (Southern Biotech, Birmingham, AL) was measured in SMG epithelial or B cells, respectively, to confirm cell viability.

### 2.5 | Immunohistochemistry and bright-field microscopy

Submandibular glands from IL-14αTG and IL-14αTG × $P2Y_2R^{-/-}$ mice were excised and placed in 4% (v/v) paraformaldehyde in PBS at 4°C for 24 hr followed by 70% (v/v) ethanol at 4°C for 24 hr. Samples were then sent to IDEXX Laboratories (Columbia, MO) where glands were embedded in paraffin, cut into 5-μm sections, and stained with hematoxylin and eosin or specific antibodies for the B cell marker B220 (Caltag Medsystems, Buckingham, United Kingdom), the T cell marker CD3 (Dako, Carpinteria, CA), or lymphotoxin-α (OriGene, Rockville, MD). Stained sections were visualized on a Zeiss Axiovert 200M inverted microscope, and images were captured using Molecular Devices MetaMorph software at the University of Missouri's Molecular Cytology Core facility.

### 2.6 | Focus score measurement

Images of whole submandibular and sublingual gland sections were generated by stitching together multiple 40× magnification bright-field images using MetaMorph software. From stitched whole gland images, the number of lymphocytic foci in each gland was counted and total gland area measurements were determined using MetaMorph software. The extent of lymphocytic infiltration in the salivary gland was assessed by calculating the focus score; a clinical measure of salivary gland inflammation defined as the number of lymphocytic foci (lymphocyte aggregates > 50 cells) per 4 $mm^2$ of tissue (Daniels et al., 2011).

### 2.7 | Saliva collection

Carbachol-stimulated saliva secretion was measured as previously described (Kayes et al., 2016). Mice were anesthetized with Avertin (0.3 mg/g body weight; Sigma-Aldrich, St. Louis, MO), and a midventral incision was made at the base of the throat to accommodate an endotracheal tube (PE50 polyethylene tubing) to prevent aspiration. Following stimulation of saliva secretion by intraperitoneal injection of carbachol (0.25 mg/kg mouse weight; Sigma-Aldrich), whole saliva was collected from the oral cavity by pipet for 15 min and placed in a preweighed Eppendorf tube.

### 2.8 | Autoantibody measurements

Following anesthetization with Avertin, blood was collected from 12-month-old IL-14αTG and IL-14αTG × $P2Y_2R^{-/-}$ mice by cardiac puncture with a 22G needle and 3-ml syringe. Whole blood (500 μl) was added to an Eppendorf tube, allowed to clot for 20 min at room temperature, and then centrifuged at 2,000 × *g* for 10 min to isolate serum. Serum concentrations of autoantibodies were measured by specific ELISA kits for mouse anti-SSA/Ro and anti-SSB/La (Alpha Diagnostic International, San Antonio, TX), per manufacturer's protocol.

### 2.9 | SDS-PAGE and Western blot analysis

Whole SMGs were homogenized in Tissue Protein Extraction Reagent (Thermo Scientific, Rockford, IL) containing protease inhibitor cocktail (Sigma-Aldrich). Samples were centrifuged at 10,000 × *g* for 5 min to pellet cellular debris, supernatants were collected, and the protein concentration was measured using a Nanodrop One spectrophotometer. Following protein concentration normalization, samples were combined 1:1 with 2× Laemmli Buffer (20 m mol $L^{-1}$ sodium phosphate, pH 7.0, 20% (v/v) glycerol, 4% (w/v) SDS, 0.01% (w/v) bromophenol blue, and 100 m mol $L^{-1}$ DTT) and subjected to Western blot analysis. Samples containing 50 μg total protein were subjected to 12% (w/v) SDS-PAGE and transferred to nitrocellulose membranes. Membranes were washed in Tris-buffered saline (pH 7.4) containing 0.1% (v/v) Tween-20 (TBST), blocked for 1 hr with 5% (w/v) non-fat dry milk in TBST, and incubated with rat anti-lymphotoxin-α (MAB749, R & D Systems, Minneapolis, MN; diluted 1:1,000 in TBST) or rabbit anti-Erk1/2 (137F5, Cell Signaling Technology, Danvers, MA; diluted 1:2,000 in TBST) antibody for 16 hr at 4°C. Membranes were then washed in TBST and incubated with horseradish peroxidase-conjugated goat anti-rabbit or goat antirat IgG antibody (Cell Signaling Technology, 1:2,000 dilution in TBST) at room temperature for 1 hr. Protein bands were visualized using enhanced chemiluminescence reagent (Thermo Scientific), detected on X-ray film, and quantified using a flat-bed scanner and LI-COR Image Studio Software.

### 2.10 | Lymphotoxin-α quantification by ELISA

Primary SMG epithelial cells were isolated from 9-month-old IL-14αTG mice, as described above, and suspended in serum-free 1:1 DMEM:Ham's F-12 media containing 50 μg/ml gentamicin. The cells were incubated for 2 hr (37°C, 95% air, 5% $CO_2$) and then treated with or without 100 μ mol $L^{-1}$ UTP for 24 hr. Cells were then pelleted by centrifugation (1,000 × *g* for 5 min), supernatant was collected, and cells were sonicated in Tissue Protein Extraction Reagent (Thermo Scientific). Cell lysates were centrifuged at 10,000 × *g* for 5 min to pellet cellular debris, and the protein concentration was measured using a Nanodrop One spectrophotometer. Lymphotoxin-α levels were measured in cell lysates and supernatants using the Mouse LTA/TNF Beta ELISA Kit (LS-F5195, LifeSpan Biosciences, Inc., Seattle, WA), per the manufacturer's protocol, and results were normalized to total protein concentration of cell lysate.

### 2.11 | Statistics

Quantitative results are presented as means ± *SEM* of data from three or more independent experiments. Statistical significance, defined as $p < .05$, was calculated by two-tailed Student's *t* test or one-way ANOVA using GraphPad Prism software.

## 3 | RESULTS

### 3.1 | $P2Y_2R$ expression and function are elevated in SMG and spleen from IL-14αTG mice, as compared to wild-type control mice

Our previous studies indicate that under homeostatic, non-inflammatory conditions $P2Y_2R$ expression and function are low in mouse SMG and are significantly upregulated during salivary gland inflammation (Ahn et al., 2000; El-Sayed et al., 2014; Schrader et al., 2005). IL-14αTG mice exhibit sialadenitis and alterations in B-cell subpopulations within the spleen at 9–12 months of age (Shen et al., 2006). To determine $P2Y_2R$ expression levels, whole SMGs and spleens from 9-month-old wild-type, IL-14αTG, and IL-14αTG × $P2Y_2R^{-/-}$ mice were subjected to RT-PCR analysis which demonstrated that $P2Y_2R$ mRNA expression is significantly increased in IL-14αTG mouse SMG ($p = .03$) and spleen ($p = .043$), as compared to age-matched wild-type samples. As expected, $P2Y_2R$ mRNA was absent in SMG and spleen from IL-14αTG × $P2Y_2R^{-/-}$ mice (Figure 1a, b).

To determine functional $P2Y_2R$ expression, primary salivary epithelial cells freshly isolated from the SMGs of 12-month-old IL-14αTG and wild-type control mice were treated with the selective $P2Y_2R$ agonist UTP (100 μ mol $L^{-1}$) and changes in intracellular $Ca^{2+}$ levels ($[Ca^{2+}]_i$) were measured. SMG epithelial cells (11 of 38 cells tested) from IL-14αTG mice displayed UTP-induced increases in $[Ca^{2+}]_i$, whereas, similar to our previous findings (El-Sayed et al., 2014; Schrader et al., 2005), UTP elicited no change in $[Ca^{2+}]_i$ in SMG epithelial cells (0 of 14 cells tested) isolated from wild-type mice (Figure 1c). UTP-induced increases in $[Ca^{2+}]_i$ also were observed in splenic B cells (4 of 7 cells tested) and SMG B cells (14 of 18 cells tested) isolated from 12-month-old IL-14αTG mice, but not in splenic B cells (0 of 22 cells tested) or SMG B cells (0 of 27 cells tested) from wild-type mice (Figure 1d). As expected, no UTP-induced changes in $[Ca^{2+}]_i$ were observed in cells isolated from IL-14αTG × $P2Y_2R^{-/-}$ mice (data not shown).

### 3.2 | $P2Y_2R$ knockout attenuates lymphocytic infiltration of the SMG in IL-14αTG mice

Lymphocyte accumulation in the salivary glands is one of several key diagnostic criteria for SS in humans that is recapitulated in IL-14αTG mice by 9 months of age (Shen et al., 2006). To investigate the role of the $P2Y_2R$ in the development of sialadenitis in IL-14αTG mice, lymphocytic infiltration was analyzed in SMGs from 9- and 12-month-old IL-14αTG and IL-14αTG × $P2Y_2R^{-/-}$ mice. As compared to SMGs of age-matched IL-14αTG mice, salivary gland inflammation was dramatically reduced in SMGs of IL-14αTG × $P2Y_2R^{-/-}$ mice, which displayed fewer lymphocytic foci at both 9 and 12 months of age (Figure 2a). Quantification of lymphocytic infiltration was performed by determining SMG focus scores. As compared to SMGs of age-matched IL-14αTG mice, the focus scores were significantly reduced in SMGs of IL-14αTG × $P2Y_2R^{-/-}$ mice at both 9 months ($p < .0001$) and 12 months of age ($p = .0002$) (Figure 2b).

In human SS patients, both B- and T-cell subpopulations have been shown to accumulate in the salivary glands (Christodoulou, Kapsogeorgou, & Moutsopoulos, 2010). As shown in Figure 3a, the lymphocytic foci in the SMG of 9-month-old IL-14αTG mice are composed of both $B220^+$ B cells and $CD3^+$ T cells and both lymphocyte populations were reduced in SMGs of age-matched IL-14αTG × $P2Y_2R^{-/-}$ mice. Quantification of immune cell infiltrates in SMGs of 9-month-old IL-14αTG, IL-14αTG × $P2Y_2R^{-/-}$, and age-matched control mice was determined by RT-PCR analysis of cDNA from whole SMGs using primers for the pan-B cell marker *CD20* and the pan-T cell marker *CD3.* Similar to results in Figure 3a, there was a significant decrease in the expression of *CD20* ($p = .0027$) and *CD3* ($p = .0039$) in SMGs from IL-14αTG × $P2Y_2R^{-/-}$, as compared to age-matched IL-14αTG mice (Figure 3b, c).

### 3.3 | $P2Y_2R$ knockout does not affect whole saliva production or anti-Ro/anti-La autoantibody production in IL-14αTG mice

To determine whether the observed attenuation of sialadenitis in IL-14αTG × $P2Y_2R^{-/-}$ mice resulted in improved salivation, carbachol-induced saliva secretion was measured in 12-month-old wild-type, IL-14αTG, and IL-14αTG × $P2Y_2R^{-/-}$ mice. As shown in Figure 4, saliva secretion was significantly reduced in IL-14αTG mice, as compared to age-matched wild-type mice ($p = .046$). However, saliva volume was not significantly different between IL-14αTG and IL-14αTG × $P2Y_2R^{-/-}$ mice ($p = .113$). Additionally, no significant difference in carbachol-induced saliva secretion was observed between wild-type and $P2Y_2R^{-/-}$ control mice (Figure S1). Although previous studies have already demonstrated that few IL-14αTG mice develop anti-Ro and/or anti-La autoantibodies (Shen et al., 2006), we nevertheless measured serum concentrations of these autoantibodies in 12-month-old IL-14αTG and IL-14αTG × $P2Y_2R^{-/-}$ mice. As anticipated, neither anti-Ro nor anti-La autoantibodies were detected in serum from IL-14αTG or IL-14αTG × $P2Y_2R^{-/-}$ mice (data not shown).

### 3.4 | Upregulation of Lymphotoxin-α in the IL-14αTG mouse SMG is attenuated by $P2Y_2R$ deletion

Previous studies have implicated Lymphotoxin-α as a key contributor to autoimmune pathologies in IL-14αTG mice (Shen et al., 2010, 2013). Because $P2Y_2R$ activation has been previously shown to induce LTA upregulation and release (Qian et al., 2016; Seye et al., 2012), we investigated whether $P2Y_2R$ knockout altered LTA levels in IL-14αTG mice. RT-PCR analysis of cDNA prepared from whole SMGs from 9-month-old IL-14αTG, IL-14αTG × $P2Y_2R^{-/-}$, wild-type, and $P2Y_2R^{-/-}$ mice revealed that LTA mRNA expression was significantly reduced in IL-14αTG × $P2Y_2R^{-/-}$ mouse SMG, as compared to IL-14αTG mouse SMG ($p = .0038$) (Figure 5a). Western analysis of SMG lysates also showed significantly reduced LTA expression in 9-month-old IL-14αTG × $P2Y_2R^{-/-}$ mouse SMG, as compared to IL-14αTG mouse SMG ($p = .0149$) (Figure 5b). Immunohistochemical analysis of LTA expression using an anti-LTA antibody showed positive LTA expression in both SMG epithelium and infiltrating lymphocytes in the SMGs of 9-month-old IL-14αTG mice that was dramatically reduced in IL-14αTG × $P2Y_2R^{-/-}$ mice (Figure 5c). Control experiments verified that LTA was strongly detected in mouse colon adenocarcinoma (positive control) and there was no staining of SMGs with secondary antibody only (Figure

S2). We further investigated whether $P2Y_2R$ activation in IL-14αTG SMG cells alters LTA expression and release. As shown in Figure 5d, UTP-mediated $P2Y_2R$ activation induced significant upregulation of LTA ($p = .0167$) in primary SMG cells from 9-month-old IL-14αTG mice, whereas no increase in LTA levels was observed in the cell supernatant.

## 4 | DISCUSSION

Despite the fact that $P2Y_2Rs$ regulate a wide range of inflammatory responses in cell types associated with SS, including immune, epithelial, and endothelial cells, the contribution of $P2Y_2Rs$ to the development of autoimmune diseases, including SS, has remained largely unexplored. Here, we provide novel evidence that the $P2Y_2R$ contributes to autoimmune sialadenitis in the IL-14α transgenic mouse model of SS (Figures 2 and 3). Consistent with previous studies that demonstrate $P2Y_2R$ upregulation in inflamed tissue (Ahn et al., 2000; Degagne et al., 2009; Schrader et al., 2005; Turner et al., 1997), the present study shows that relative to wild-type mice, $P2Y_2Rs$ are up-regulated in whole SMG and spleen and isolated SMG epithelial cells, SMG B cells, and splenic B cells from IL-14αTG mice (Figure 1). We also observed a significant reduction in LTA expression in the SMGs of IL-14αTG × $P2Y_2R^{-/-}$ mice, as compared to IL-14αTG mice, and found that UTP-mediated $P2Y_2R$ activation induced significant upregulation of LTA in primary SMG cells from IL-14αTG mice (Figure 5). These results are consistent with previous studies indicating that the $P2Y_2R$ regulates transcriptional activation of *LTA* and that the loss of LTA expression attenuates sialadenitis in IL-14αTG mice (Seye et al., 2012; Shen et al., 2009, 2010, 2013).

The immune pathogenesis leading to the destruction of salivary glands, hyposalivation, and development of autoantibodies in SS is not fully understood, but involves infiltration of B and T lymphocytes to perivascular or periductal locations in salivary glands (Christodoulou et al., 2010; Mavragani & Moutsopoulos, 2014). Minor salivary gland biopsies from human SS patients and whole salivary glands dissected from SS mouse models exhibit temporal changes in lymphocyte populations during disease progression where TH1 cells are initially recruited followed by B cells (Christodoulou et al., 2010; Nguyen, Cha, & Peck, 2007; Roescher et al., 2012). Although the role of T cells in the development of the SS-I ike phenotype in IL-14αTG mice is unknown, here we demonstrate that $P2Y_2R$ knockout reduces accumulation of T cells in the SMG of IL-14αTG mice (Figure 3a, c). $P2Y_2R$ knockout has been shown to reduce proliferation of cytokine-secreting autoreactive T cells in a mouse model of autoimmune uveitis (Relvas et al., 2015). We have previously demonstrated that $P2Y_2R$ upregulation is an early response in thymocyte maturation into T cells (Koshiba et al., 1997) and ATP has been shown to stimulate T-cell proliferation and migration (Trabanelli et al., 2012). Whereas T cells predominate in salivary gland biopsies from SS patients with mild sialadenitis, B cells predominate in SS patients with severe sialadenitis (Christodoulou et al., 2010). Similarly, in the NOD mouse model of SS, early-stage lymphocytic foci in salivary glands are predominately composed of $CD3^+$ T cells with later stage foci primarily consisting of $B220^+$ B cells (Nguyen et al., 2007).

Recent studies suggest that B-cell hyperactivity is central to the SS phenotype (Ambrus, Suresh, & Peck, 2016; Nguyen et al., 2007; Shen et al., 2016). Marginal zone (MZ)-like B cells, memory B cells, and plasma cells are present within salivary glands of SS patients

(Daridon et al., 2006;Szyszko et al., 2011). Similarly, IL-14αTG mice have increased numbers of MZ B cells, germinal center (GC) B cells, and plasma cells in the spleen, as compared to wild-type mice (Shen et al., 2006). B-cell contributions to SS-like pathologies in IL-14αTG mice were highlighted in a recent study where IL-14αTG × CD19Cre.RBP-J $^{-/-}$ mice in which MZ B cells were depleted exhibited significantly reduced serum autoantibody levels, as compared to age-matched IL-14αTG mice, as well as salivary gland histology and saliva secretion similar to non-diseased control mice (Shen et al., 2016). The functional role of $P2Y_2$Rs in B cells has not been previously investigated. Our data demonstrate the novel finding that $P2Y_2$R activity (i.e., UTP-induced increases in $[Ca^{2+}]_i$) is expressed in B cells from 9-month-old IL-14αTG mouse SMG and spleen, but is absent in B cells isolated from age-matched wild-type mice (Figure 1). Additionally, we found that global knockout of the $P2Y_2$R in IL-14αTG mice significantly reduced B-cell accumulation in the SMG (Figures 2 and 3). However, it appears that attenuated sialadenitis following $P2Y_2$R knockout is not enough to prevent hyposalivation in IL-14αTG mice, as there was no significant difference in saliva production between IL-14αTG and IL-14αTG × $P2Y_2R^{-/-}$ mice (Figure 4). Previous studies have demonstrated that salivary gland hypofunction precedes sialadenitis during the development of SS-like pathologies in IL-14αTG mice, suggesting that salivary gland hypofunction in IL-14αTG mice is regulated separately from sialadenitis, perhaps through increased peri-acinar IgM deposition (Shen et al., 2009).

In addition to immune cells, epithelial cells may also contribute to SS pathogenesis by modulating immune reactions in inflammatory lesions of SS (Moutsopoulos, 1994). Studies of minor gland biopsies from SS patients and salivary glands from SS mouse models note that epithelial cells surrounding sites of intense inflammation express high levels of immunoactive proteins that promote immune cell adhesion and activation (Manoussakis & Kapsogeorgou, 2010;Saito et al., 1993). Our previous findings indicate that, under non-inflammatory conditions, $P2Y_2$R-mediated increases in $[Ca^{2+}]_i$ are absent in freshly isolated SMG cells, but are significantly increased in SMG cells under inflammatory conditions, including SMG duct ligation- or autoimmune-associated sialadenitis (Ahn et al., 2000; El-Sayed et al., 2014; Schrader et al., 2005). Here, we demonstrate that $P2Y_2$R expression and function are elevated in isolated SMG epithelial cells from IL-14αTG mice, as compared to wild-type mice (Figure 1), and LTA is expressed in SMG epithelium from IL-14αTG mice (Figure 5c). Furthermore, UTP-induced activation of the $P2Y_2$R upregulates LTA expression in primary SMG cells from IL-14αTG mice, whereas no increase in LTA levels was observed in the cell supernatant (Figure 5d). These data suggest that $P2Y_2$R activation in IL-14αTG salivary gland cells increases LTA protein expression rather than secretion, although previous studies have demonstrated that $P2Y_2$R activation can increase both expression and release of LTA in other cell types (Qian et al., 2016; Seye et al., 2012).

Lymphotoxin-α (also known as TNF-β) exists as a homotrimer that binds TNF receptors or as a heterotrimer in a 1:2 stoichiometry with lymphotoxin β (LTα1β2) that binds lymphotoxin-β receptors to induce cellular responses (Browning et al., 1995). Although many ligands in the lymphotoxin/TNF pathway have overlapping signaling roles, it has become clear that lymphotoxin signaling is a key regulator of immune cell interactions and development of lymphoid tissues (Gommerman & Browning, 2003). LTA knockout mice fail to develop secondary lymphoid tissues, including peripheral lymph nodes and Peyer's

patches, and have an aberrant organization of B and T cells within the spleen (De Togni et al., 1994). Furthermore, inhibition of lymphotoxin signaling using function-blocking anti-lymphotoxin-β receptor antibodies prevents germinal center formation in response to immunization with foreign antigens (Mackay, Majeau, Lawton, Hochman, & Browning, 1997) and has been shown to reverse the SS-I ike phenotype in non-obese diabetic (NOD) mice by reducing sialadenitis and improving saliva secretion (Gatumu et al., 2009). Previous studies indicate that IL-14αTG mice exhibit increased LTA levels in the salivary glands, saliva, spleen, and serum, as compared to age-matched C57BL/6 control mice, and LTA knockout in IL-14αTG mice attenuates sialadenitis and enhances saliva secretion (Shen et al., 2010, 2013). SS patients also exhibit increased LTA levels in saliva and serum, as compared to healthy individuals, and normal salivary gland tissue isolated from healthy individuals and treated with LTA exhibits significantly reduced carbachol-i nduced A$[Ca^{2+}]_i$ similar to salivary tissue isolated from SS patients (Teos et al., 2015). These studies highlight the relevance of local LTA production to salivary hypofunction in SS. Interestingly, genomewide DNA methylation studies have identified numerous sites within the *LTA* gene that are differentially methylated in SS patients compared to healthy patients or within SS patient subgroups (i.e., SS patients with high fatigue vs SS patients with low fatigue), suggesting that *LTA* may be a specific target of epigenetic regulation in SS (Altorok et al., 2014; Braekke Norheim et al., 2016). Observations from our laboratory have identified two significantly hypomethylated sites in the *LTA* gene in 9-month-old IL-14αTG × $P2Y_2R^{-/-}$ mouse SMG, as compared to age-matched IL-14αTG mouse SMG (Figure S3). However, decreased DNA methylation is generally associated with increased gene expression, suggesting that the $P2Y_2R$ regulates LTA expression through a different mechanism. Nevertheless, the data presented here suggest that the $P2Y_2R$ contributes to autoimmune sialadenitis in the IL-14αTG mouse model of SS and further investigation of this pathway should illuminate novel approaches to reduce chronic salivary gland inflammation and subsequent tissue damage in humans with SS.

## Supplementary Material

Refer to Web version on PubMed Central for supplementary material.

## ACKNOWLEDGEMENTS

This work was supported by the National Institute of Dental & Craniofacial Research grants R01DE007389 and R01DE023342.

Funding information

National Institute of Dental and Craniofacial Research, Grant/Award Number: R01DE007389 and R01DE023342

## REFERENCES

Ahn JS, Camden JM, Schrader AM, Redman RS, & Turner JT (2000). Reversible regulation of $P2Y_2$ nucleotide receptor expression in the duct-ligated rat submandibular gland. American Journal of Physiology-Cell Physiology, 279, C286–C294. 10.1152/ajpcell.2000.279.2.C286 [PubMed: 10912994]

Ajit D, Woods LT, Camden JM, Thebeau CN, El-Sayed FG, Greeson GW, … Weisman GA (2014). Loss of $P2Y_2$ nucleotide receptors enhances early pathology in the TgCRND8 mouse model of

Alzheimer's disease. Molecular Neurobiology, 49, 1031–1042. 10.1007/s12035-013-8577-5 [PubMed: 24193664]

Altorok N, Coit P, Hughes T, Koelsch KA, Stone DU, Rasmussen A, … Sawalha AH (2014). Genome-wide DNA methylation patterns in naive CD4+ T cells from patients with primary Sjögren's syndrome. Arthritis & Rheumatology, 66, 731–739. 10.1002/art.38264 [PubMed: 24574234]

Ambrus JL, Suresh L, & Peck A (2016). Multiple roles for B-lymphocytes in Sjögren's syndrome. Journal of Clinical Medicine, 5, E87 10.3390/jcm5100087 [PubMed: 27740602]

Bagchi S, Liao Z, Gonzalez FA, Chorna NE, Seye CI, Weisman GA, & Erb L (2005). The $P2Y_2$ nucleotide receptor interacts with $\alpha_V$ integrins to activate $G_O$ and induce cell migration. Journal of Biological Chemistry, 280, 39050–39057. 10.1074/jbc.M504819200 [PubMed: 16186116]

Braekke Norheim K, Imgenberg-Kreuz J, Jonsdottir K, Janssen EA, Syvanen AC, Sandling JK, … Omdal R (2016). Epigenome-wide DNA methylation patterns associated with fatigue in primary Sjögren's syndrome. Rheumatology, 55, 1074–1082. 10.1093/rheumatology/kew008 [PubMed: 26966136]

Browning JL, Dougas I, Ngam-ek A, Bourdon PR, Ehrenfels BN, Miatkowski K, … Meier W (1995). Characterization of surface lymphotoxin forms. Use of specific monoclonal antibodies and soluble receptors. The Journal of Immunology, 154, 33–46. [PubMed: 7995952]

Cha S, Nagashima H, Brown VB, Peck AB, & Humphreys-Beher MG (2002). Two NOD Idd-associated intervals contribute synergistically to the development of autoimmune exocrinopathy (Sjögren's syndrome) on a healthy murine background. Arthritis and Rheumatism, 46, 1390–1398. 10.1002/art.10258 [PubMed: 12115247]

Christodoulou MI, Kapsogeorgou EK, & Moutsopoulos HM (2010). Characteristics of the minor salivary gland infiltrates in Sjögren's syndrome. Journal of Autoimmunity, 34, 400–407. 10.1016/j.jaut.2009.10.004 [PubMed: 19889514]

Daniels TE, Cox D, Shiboski CH, Schiodt M, Wu A, Lanfranchi H, … Greenspan JS (2011). Associations between salivary gland histopathologic diagnoses and phenotypic features of Sjögren's syndrome among 1,726 registry participants. Arthritis and Rheumatism, 63, 2021–2030. 10.1002/art.30381 [PubMed: 21480190]

Daridon C, Pers JO, Devauchelle V, Martins-Carvalho C, Hutin P, Pennec YL, … Youinou P (2006). Identification of transitional type II B cells in the salivary glands of patients with Sjögren's syndrome. Arthritis and Rheumatism, 54, 2280–2288. 10.1002/(ISSN)1529-0131 [PubMed: 16802367]

De Togni P, Goellner J, Ruddle NH, Streeter PR, Fick A, Mariathasan S, … Russell JH (1994). Abnormal development of peripheral lymphoid organs in mice deficient in lymphotoxin. Science, 264, 703–707. 10.1126/science.8171322 [PubMed: 8171322]

Degagne E, Grbic DM, Dupuis AA, Lavoie EG, Langlois C, Jain N, … Gendron FP (2009). $P2Y_2$ receptor transcription is increased by NF-κB and stimulates cyclooxygenase-2 expression and PGE2 released by intestinal epithelial cells. The Journal of Immunology, 183, 4521–4529. 10.4049/jimmunol.0803977 [PubMed: 19734210]

El-Sayed FG, Camden JM, Woods LT, Khalafalla MG, Petris MJ, Erb L, & Weisman GA (2014). $P2Y_2$ nucleotide receptor activation enhances the aggregation and self-organization of dispersed salivary epithelial cells. American Journal of Physiology-Cell Physiology, 307, C83–C96. 10.1152/ajpcell.00380.2013 [PubMed: 24760984]

Gaffney PM, Kearns GM, Shark KB, Ortmann WA, Selby SA, Malmgren ML, … Behrens TW (1998). A genome-wide search for susceptibility genes in human systemic lupus erythematosus sib-pair families. Proceedings of the National Academy of Sciences USA, 95, 14875–14879. 10.1073/pnas.95.25.14875

Gatumu MK, Skarstein K, Papandile A, Browning JL, Fava RA, & Bolstad AI (2009). Blockade of lymphotoxin-β receptor signaling reduces aspects of Sjögren's syndrome in salivary glands of non-obese diabetic mice. Arthritis Research & Therapy, 11, R24 10.1186/ar2617 [PubMed: 19222863]

Gommerman JL, & Browning JL (2003). Lymphotoxin/light, lymphoid microenvironments and autoimmune disease. Nature Reviews Immunology, 3, 642–655. 10.1038/nri1151

Kayes TD, Weisman GA, Camden JM, Woods LT, Bredehoeft C, Downey EF, … Braley-Mullen H (2016). New murine model of early onset autoimmune thyroid disease/hypothyroidism and autoimmune exocrinopathy of the salivary gland. The Journal of Immunology, 197, 2119–2130. 10.4049/jimmunol.1600133 [PubMed: 27521344]

Koshiba M, Apasov S, Sverdlov V, Chen P, Erb L, Turner JT, … Sitkovsky MV (1997). Transient up-regulation of $P2Y_2$ nucleotide receptor mRNA expression is an immediate early gene response in activated thymocytes. Proceedings of the National Academy of Sciences USA, 94, 831–836. 10.1073/pnas.94.3.831

Lustig KD, Erb L, Landis DM, Hicks-Taylor CS, Zhang X, Sportiello MG, & Weisman GA (1992). Mechanisms by which extracellular ATP and UTP stimulate the release of prostacyclin from bovine pulmonary artery endothelial cells. Biochimica et Biophysica Acta, 1134, 61–72. 10.1016/0167-4889(92)90028-A [PubMed: 1311959]

Mackay F, Majeau GR, Lawton P, Hochman PS, & Browning JL (1997). Lymphotoxin but not tumor necrosis factor functions to maintain splenic architecture and humoral responsiveness in adult mice. European Journal of Immunology, 27, 2033–2042. 10.1002/(ISSN)1521-4141 [PubMed: 9295042]

Manoussakis MN, & Kapsogeorgou EK (2010). The role of intrinsic epithelial activation in the pathogenesis of Sjögren's syndrome. Journal of Autoimmunity, 35, 219–224. 10.1016/j.jaut.2010.06.011 [PubMed: 20685080]

Mavragani CP, & Moutsopoulos HM (2014). Sjögren syndrome. CMAJ: Canadian Medical Association Journal, 186, E579–E586. 10.1503/cmaj.122037 [PubMed: 24566651]

Moutsopoulos HM (1994). Sjögren's syndrome: Autoimmune epithelitis. Clinical Immunology and Immunopathology, 72, 162–165. 10.1006/clin.1994.1123 [PubMed: 8050187]

Nguyen CQ, Cha SR, & Peck AB (2007). Sjögren's syndrome (SJS)-like disease of mice: The importance of B lymphocytes and autoantibodies. Frontiers in Bioscience, 12, 1767–1789. 10.2741/2187 [PubMed: 17127420]

Qian S, Hoggatt A, Jones-Hall YL, Ware CF, Herring P, & Seye CI (2016). Deletion of $P2Y_2$ receptor reveals a role for Lymphotoxin-α in fatty streak formation. Vascular Pharmacology, 85, 11–20. 10.1016/j.vph.2016.06.001 [PubMed: 27355755]

Ratchford AM, Baker OJ, Camden JM, Rikka S, Petris MJ, Seye CI, … Weisman GA (2010). $P2Y_2$ nucleotide receptors mediate metalloprotease-dependent phosphorylation of epidermal growth factor receptor and ErbB3 in human salivary gland cells. Journal of Biological Chemistry, 285, 7545–7555. 10.1074/jbc.M109.078170 [PubMed: 20064929]

Relvas LJ, Makhoul M, Dewispelaere R, Caspers L, Communi D, Boeynaems JM, … Willermain F (2015). $P2Y_2R$ deficiency attenuates experimental autoimmune uveitis development. PLoS ONE, 10, e0116518 10.1371/journal.pone.0116518 [PubMed: 25692550]

Roescher N, Lodde BM, Vosters JL, Tak PP, Catalan MA, Illei GG, & Chiorini JA (2012). Temporal changes in salivary glands of non-obese diabetic mice as a model for Sjögren's syndrome. Oral Diseases, 18, 96–106. 10.1111/jM601-0825.2011.01852.x [PubMed: 21914088]

Saito I, Terauchi K, Shimuta M, Nishiimura S, Yoshino K, Takeuchi T, … Miyasaka N (1993). Expression of cell adhesion molecules in the salivary and lacrimal glands of Sjögren's syndrome. Journal of Clinical Laboratory Analysis, 7, 180–187. 10.1002/(ISSN)1098-2825 [PubMed: 8509947]

Schrader AM, Camden JM, & Weisman GA (2005). $P2Y_2$ nucleotide receptor up-regulation in submandibular gland cells from the NOD. B10 mouse model of Sjögren's syndrome. Archives of Oral Biology, 50, 533–540. 10.1016/j.archoralbio.2004.11.005 [PubMed: 15848146]

Seye CI, Agca Y, Agca C, & Derbigny W (2012). $P2Y_2$ receptor-mediated Lymphotoxin-α secretion regulates intercellular cell adhesion molecule-1 expression in vascular smooth muscle cells. Journal of Biological Chemistry, 287, 10535–10543. 10.1074/jbc.M111.313189 [PubMed: 22298782]

Seye CI, Yu N, Gonzalez FA, Erb L, & Weisman GA (2004). The $P2Y_2$ nucleotide receptor mediates vascular cell adhesion molecule-1 expression through interaction with VEGF receptor-2 (KDR/Flk-1). Journal of Biological Chemistry, 279, 35679–35686. 10.1074/jbc.M401799200 [PubMed: 15175347]

Shen L, Gao C, Suresh L, Xian Z, Song N, Chaves LD, … Ambrus JL Jr (2016). Central role for marginal zone B cells in an animal model of Sjögren's syndrome. Clinical Immunology, 168, 30–36. 10.1016/j.clim.2016.04.008 [PubMed: 27140729]

Shen L, Suresh L, Li H, Zhang C, Kumar V, Pankewycz O, & Ambrus JL Jr (2009). IL-14α, the nexus for primary Sjögren's disease in mice and humans. Clinical Immunology, 130, 304–312. 10.1016/j.clim.2008.10.006 [PubMed: 19038581]

Shen L, Suresh L, Malyavantham K, Kowal P, Xuan J, Lindemann MJ, & Ambrus JL Jr (2013). Different stages of primary Sjögren's syndrome involving lymphotoxin and type 1 IFN. The Journal of Immunology, 191, 608–613. 10.4049/jimmunol.1203440 [PubMed: 23772034]

Shen L, Suresh L, Wu J, Xuan J, Li H, Zhang C, … Ambrus JL Jr (2010). A role for lymphotoxin in primary Sjögren's disease. The Journal of Immunology, 185, 6355–6363. 10.4049/jimmunol.1001520 [PubMed: 20952683]

Shen L, Zhang C, Wang T, Brooks S, Ford RJ, Lin-Lee YC, … Ambrus JL Jr (2006). Development of autoimmunity in IL-14α-transgenic mice. The Journal of Immunology, 177, 5676–5686. 10.4049/jimmunol.177.8.5676 [PubMed: 17015757]

Shiboski SC, Shiboski CH, Criswell L, Baer A, Challacombe S, Lanfranchi H, … Daniels T (2012). American College of Rheumatology classification criteria for Sjögren's syndrome: A data-driven, expert consensus approach in the Sjögren's International Collaborative Clinical Alliance cohort. Arthritis Care & Research, 64, 475–487. 10.1002/acr.21591 [PubMed: 22563590]

Szyszko EA, Brokstad KA, Oijordsbakken G, Jonsson MV, Jonsson R, & Skarstein K (2011). Salivary glands of primary Sjögren's syndrome patients express factors vital for plasma cell survival. Arthritis Research & Therapy, 13, R2 10.1186/ar3220 [PubMed: 21214903]

Teos LY, Zhang Y, Cotrim AP, Swaim W, Won JH, Ambrus J, … Alevizos I (2015). $IP_3R$ deficit underlies loss of salivary fluid secretion in Sjögren's syndrome. Scientific Reports, 5, 13953 10.1038/srep13953 [PubMed: 26365984]

Trabanelli S, Ocadlikova D, Gulinelli S, Curti A, Salvestrini V, Vieira RP, ... Lemoli RM (2012). Extracellular ATP exerts opposite effects on activated and regulatory $CD4^+$ T cells via purinergic P2 receptor activation. The Journal of Immunology, 189, 1303–1310. 10.4049/jimmunol.1103800 [PubMed: 22753942]

Turner JT, Weisman GA, & Camden JM (1997). Upregulation of $P2Y_2$ nucleotide receptors in rat salivary gland cells during short-term culture. American Journal of Physiology, 273, C1100–C1107. 10.1152/ajpcell.1997.273.3.C1100 [PubMed: 9316432]

Woods LT, Camden JM, Batek JM, Petris MJ, Erb L, & Weisman GA (2012). P2X7 receptor activation induces inflammatory responses in salivary gland epithelium. American Journal of Physiology-Cell Physiology, 303, C790–C801. 10.1152/ajpcell.00072.2012 [PubMed: 22875784]

Woods LT, Camden JM, El-Sayed FG, Khalafalla MG, Petris MJ, Erb L, & Weisman GA (2015). Increased expression of TGF-β signaling components in a mouse model of fibrosis induced by submandibular gland duct ligation. PLoS ONE, 10, e0123641 10.1371/joumal.pone.0123641 [PubMed: 25955532]

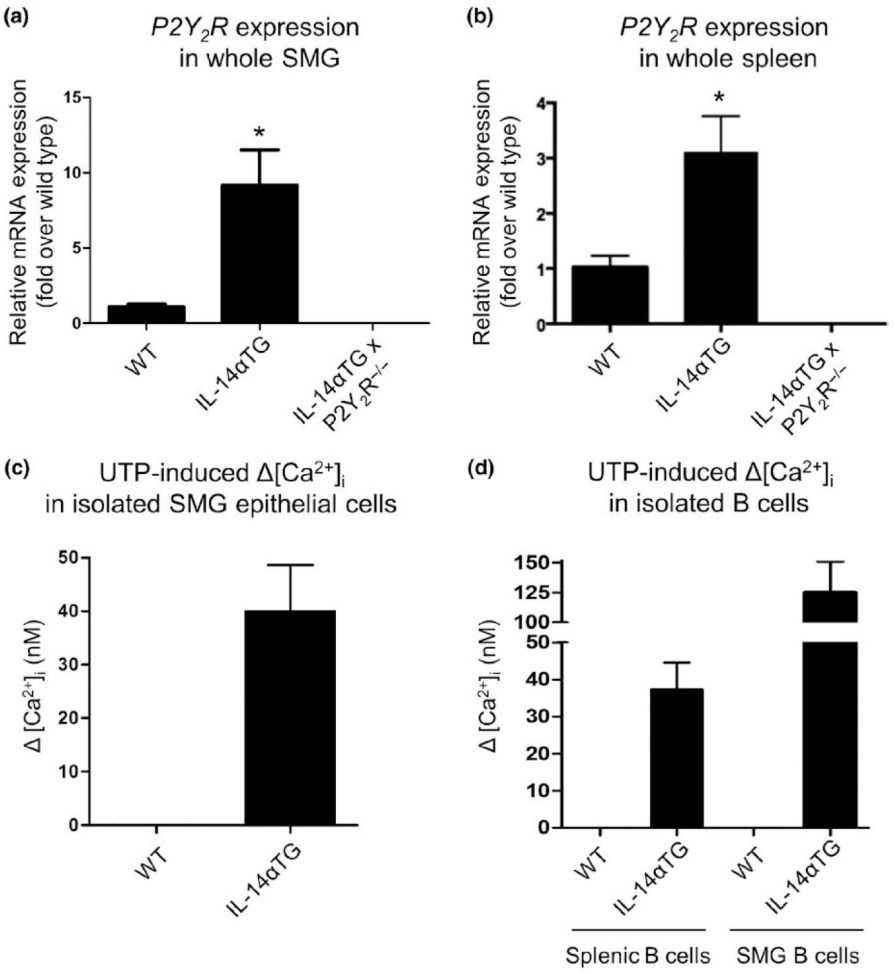


**FIGURE 1.**

Analysis of *P2Y$_2$R* expression or P2Y$_2$R function in submandibular gland (SMG), spleen, and isolated SMG epithelial and B cells from IL-14αTG and wild-type mice. The RT-PCR analysis was performed with cDNA prepared from (a) whole SMG and (b) the whole spleen from 9-month-old wild-type (WT), IL-14αTG, and IL-14αTG × P2Y$_2$R$^{-/-}$ mice. Data represent means ± *SEM* for SMGs from wild-type ($n = 5$), IL-14αTG ($n = 8$), and IL-14αTG × P2Y$_2$R$^{-/-}$ ($n = 6$) mice and spleens from wild-type ($n = 3$), IL-14αTG ($n = 4$), and IL-14αTG × P2Y$_2$R$^{-/-}$ ($n = 6$) mice, where * indicates $p < .05$. To determine functional P2Y$_2$R expression, changes in [Ca$^{2+}$]$_i$ in response to the P2Y$_2$R agonist UTP (100 μ mol L$^{-1}$) were measured in freshly isolated (c) epithelial cells from SMGs and (d) B cells from the spleens or SMGs of 12-month-old IL-14αTG and wild-type control mice. Data are means ± *SEM* of UTP-induced Δ[Ca$^{2+}$]$_i$ in pooled SMG epithelial cells from five wild-type or IL-14αTG mice or pooled splenic or SMG B cells from nine wild-type or three IL-14αTG mice

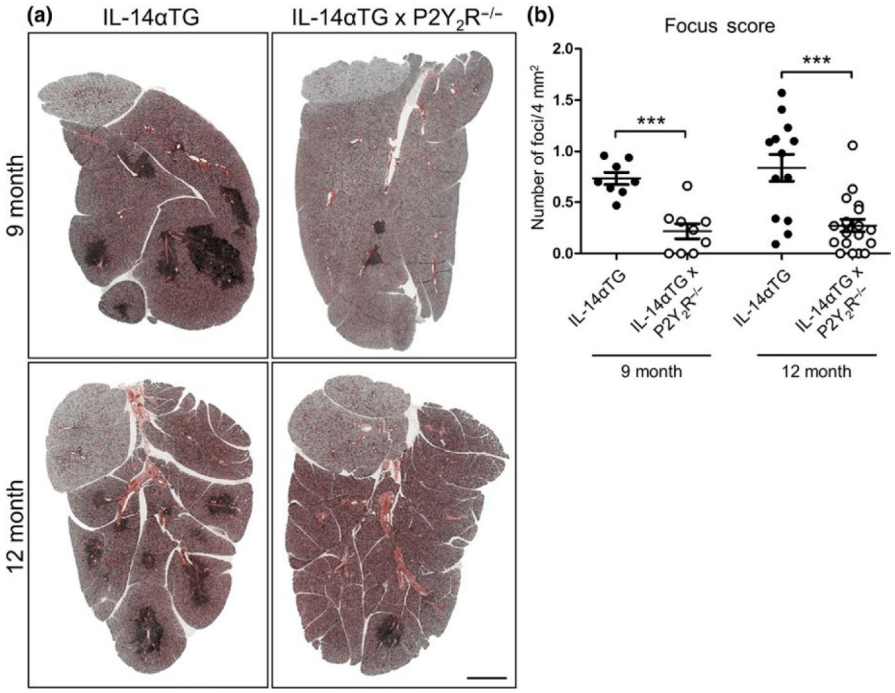


**FIGURE 2.**

Histological assessment submandibular gland (SMG) inflammation in IL-14αTG and IL-14αTG × $P2Y_2R^{-/-}$ mice. (a) Hematoxylin and eosin staining of SMGs from 9-month-old (upper panels) and 12-month-old (lower panels) IL-14αTG (left) and IL-14αTG × $P2Y_2R^{-/-}$ (right) mice; scale bar = 1 mm. (b) Quantification of lymphocyte focus score (# of lymphocytic foci/4 $mm^2$ gland area) in SMGs from 9- and 12-month-old IL-14αTG and IL-14αTG × $P2Y_2R^{-/-}$ mice. Data represent means ± *SEM* for SMGs from IL-14αTG ($n$ = 8) and IL-14αTG × $P2Y_2R^{-/-}$ ($n$ = 9) mice at 9 months of age and SMGs from IL-14αTG ($n$ = 13) and IL-14αTG × $P2Y_2R^{-/-}$ ($n$ = 19) mice at 12 months of age, where *** indicates $p < .001$

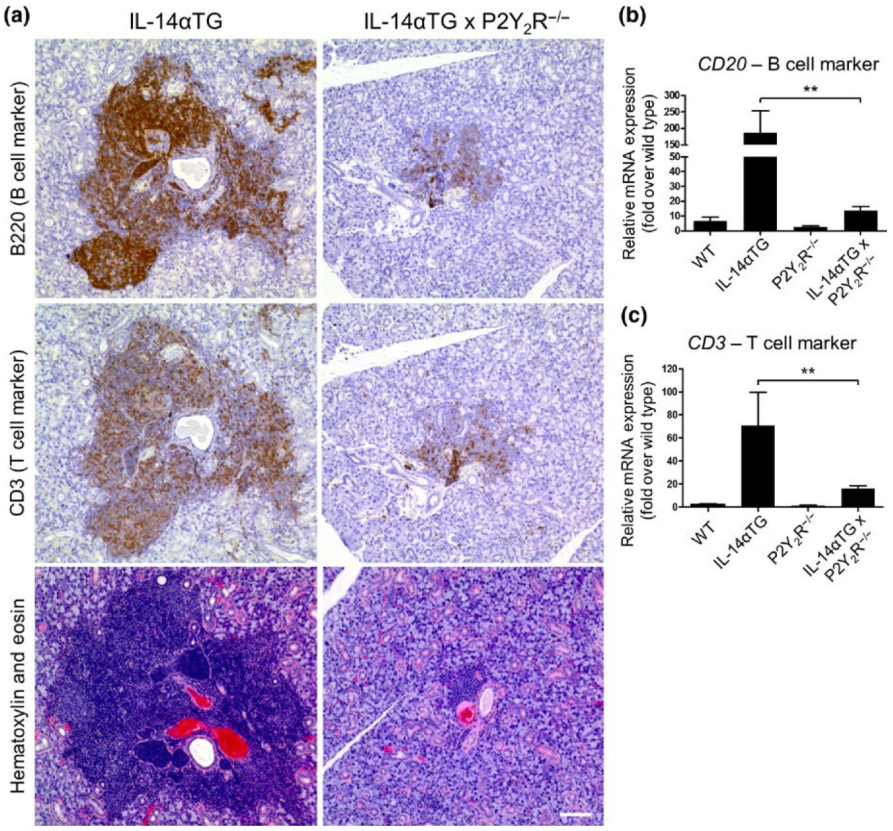


**FIGURE 3.**

Lymphocytic foci in the submandibular gland (SMG) of IL-14αTG and IL-14αTG × $P2Y_2R^{-/-}$ mice are composed of B and T cells. (a) Serial 5-μm sections of paraffin-embedded SMGs from 9-month-old IL-14αTG and IL-14αTG × $P2Y_2R^{-/-}$ mice were subjected to immunostaining for the B cell marker B220 (top panels), the T cell marker CD3 (middle panels) or hematoxylin and eosin staining (bottom panels). Images are representative of similar results for $n = 3$ mice for each genotype; scale bar = 100 μm. cDNA derived from whole SMGs of 9-month-old mice was utilized for RT-PCR analysis to determine mRNA expression of (b) the B cell marker *CD20* and (c) the T cell marker *CD3.* Data represent means ± *SEM* for SMGs of wild-type ($n = 5$), IL-14αTG ($n = 7$), $P2Y_2R^{-/-}$ ($n = 7$), and IL-14αTG × $P2Y_2R^{-/-}$ ($n = 20$) mice, where ** indicates $p < .01$

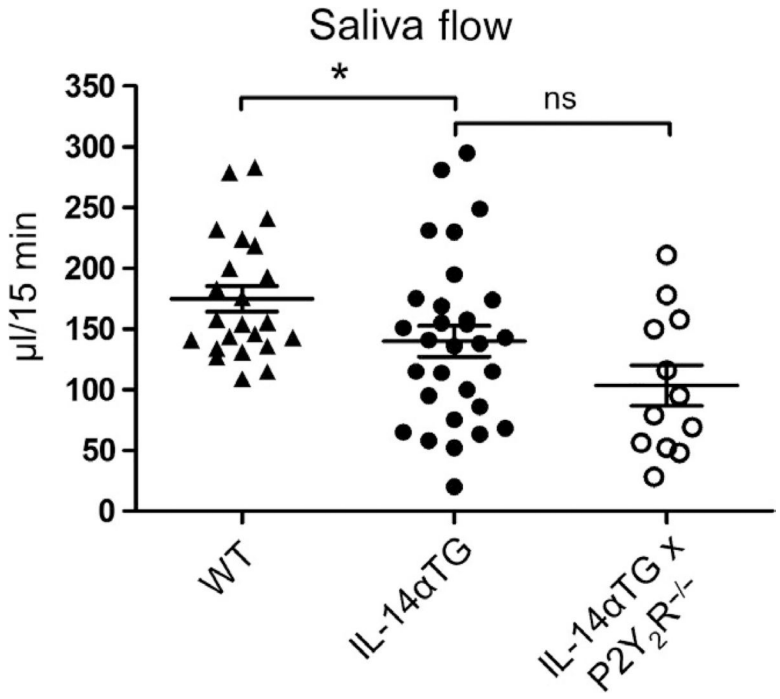


**FIGURE 4.**

Analysis of saliva secretion. Following intraperitoneal injection of carbachol (0.25 mg/kg mouse weight), the whole saliva was collected from the oral cavity of 12-month-old wild-type C57BL/6, IL-14αTG, and IL-14αTG × $P2Y_2R^{-/-}$ mice. Data represent means ± *SEM* for wild-type ($n = 23$), IL-14αTG ($n = 30$), and IL-14αTG × $P2Y_2R^{-/-}$ ($n = 12$) mice, where * indicates $p < .05$ and ns indicates no significance

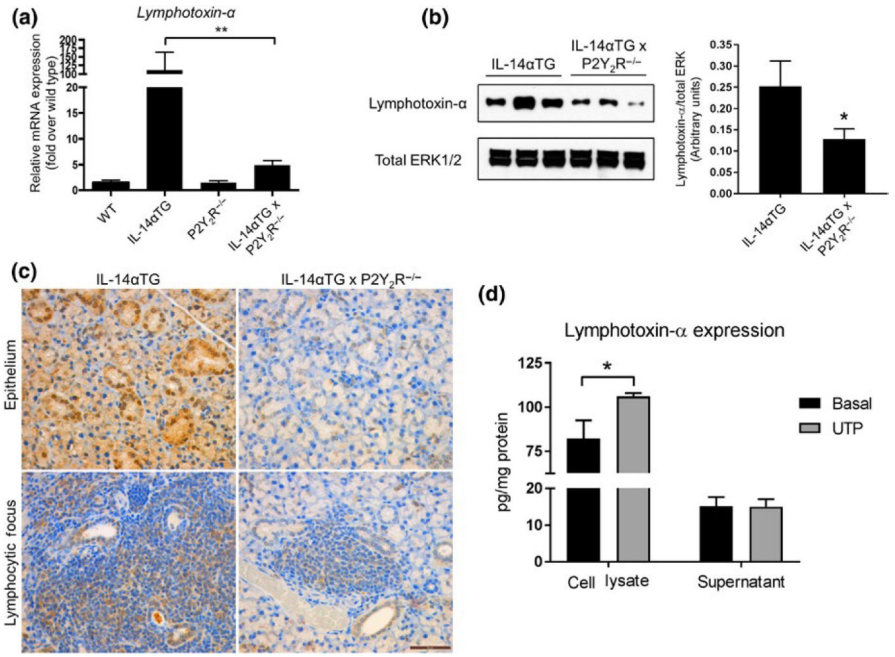


**FIGURE 5.**

Lymphotoxin-α expression in submandibular glands (SMGs) from IL-14αTG, IL-14αTG × $P2Y_2R^{-/-}$, wild-type C57BL/6, and $P2Y_2R^{-/-}$ mice. Lymphotoxin-α mRNA expression was determined by (a) RT-PCR analysis of cDNA derived from whole SMGs of 9-month-old mice. Data are means ± *SEM* for wild-type ($n = 5$), IL-14αTG ($n = 8$), $P2Y_2R^{-/-}$ ($n = 7$), and IL-14αTG × $P2Y_2R^{-/-}$ ($n = 18$) mice, where ** indicates $p < .01$. (b) Western analysis and quantification of Lymphotoxin-α protein expression in SMG lysates from 9-month-old mice. Data are means ± *SEM* for IL-14αTG ($n = 11$) and IL-14αTG × $P2Y_2R^{-/-}$ ($n = 11$) mice, where * indicates $p < .05$. (c) Immunohistochemical analysis of Lymphotoxin-α expression in epithelial cells (top panels) and lymphocytic foci (bottom panels) in SMGs from 9-month-old IL-14αTG mice (left panels) and age-matched IL-14αTG × $P2Y_2R^{-/-}$ mice (right panels). Immunohistochemistry images are representative of $n = 6$ samples for each mouse genotype; scale bar = 50 μm. (d) Primary SMG cells from 9-month-old IL-14αTG mice were treated with (gray bars) or without (black bars) 100 μ mol $L^{-1}$ UTP for 24 hr, and Lymphotoxin-α expression in cell lysates and supernatants was determined by ELISA. Data are means ± *SEM* for IL-14αTG mice from $n = 3$ experiments, where * indicates $p < .05$